Differential scanning calorimetry, x-ray diffraction and 19 F nuclear magnetic resonance investigations of the crystallization of InF 3 -based glasses

R. W. A. Franco, C. C. Tambelli, C. J. Magon, J. P. Donoso, Y. Messaddeq, S. J. L. Ribeiro, and M. Poulain

Citation: The Journal of Chemical Physics **109**, 2432 (1998); doi: 10.1063/1.476812
View online: http://dx.doi.org/10.1063/1.476812
View Table of Contents: http://scitation.aip.org/content/aip/journal/jcp/109/6?ver=pdfcov
Published by the AIP Publishing

Differential scanning calorimetry, x-ray diffraction and ^{19}F nuclear magnetic resonance investigations of the crystallization of InF_3-based glasses

R. W. A. Franco, C. C. Tambelli, C. J. Magon, and J. P. Donoso
Instituto de Física de São Carlos, Universidade de São Paulo, P.O. Box 369, 13560-970 São Carlos, SP, Brazil

Y. Messaddeq and S. J. L. Ribeiro
Instituto de Química, Unesp, PO Box 355, 14800-900 Araraquara, SP, Brazil

M. Poulain
Laboratoire des Matériaux Photoniques, Université de Rennes, Campus Beaulieu, F-35042 Rennes, France

(Received 3 December 1997; accepted 12 March 1998)

Results of differential scanning calometry (DSC), x-ray diffraction (XRD), and ^{19}F nuclear magnetic resonance (NMR) of InF_3-based glasses, treated at different temperatures, ranging from glass transition temperature (T_g) to crystallization temperature (T_c), are reported. The main features of the experimental results are as follows. DSC analysis emphasizes several steps in the crystallization process. Heat treatment at temperatures above T_g enhances the nucleation of the first growing phases but has little influence on the following ones. XRD results show that several crystalline phases are formed, with solid state transitions when heated above 680 K. The ^{19}F NMR results show that the spin–lattice relaxation, for the glass samples heat treated above 638 K, is described by two time constants. For samples treated below this temperature a single time constant T_1 was observed. Measurements of the ^{19}F spin–lattice relaxation time (T_1), as a function of temperature, made possible the identification of the mobile fluoride ions. The activation energy, for the ionic motion, in samples treated at crystallization temperature was found to be 0.18 ± 0.01 eV. © *1998 American Institute of Physics.* [S0021-9606(98)51323-2]

I. INTRODUCTION

Fluoride glasses are receiving considerable attention, motivated by their potential importance for advanced optical components.[1,2] The knowledge of the crystallization behavior of these glasses has a direct technological interest because of their application as optical fibers or laser materials. Numerous crystallization and devitrification studies, including isothermal and nonisothermal methods, have been implemented on fluorozirconate glasses using x-ray diffractometry, thermal analysis (DTA or DSC), optical microscopy, scanning electron microscopy and Raman spectroscopy.[3–10] More recently, crystallization kinetics parameters of InF_3 glasses have been determined by DSC.[11,12]

This paper reports DSC, XRD, and NMR studies of simple InF_3-based glasses, related to crystallization processes occurring after the thermal treatment of the samples at different temperatures, ranging from glass transition temperature (T_g) to crystallization temperature (T_c).

II. EXPERIMENT

Glasses with general compositions (mol %) $40InF_3$–$20ZnF_2$–$20SrF_2$–$20BaF_2$ were prepared by melting the appropriate fluorides mixtures in Pt tubes at 850 °C. They were cast on a brass mold, preheated at T_g temperature, annealed for 2 h and cooled to room temperature. DSC experiments were performed with about 10 mg of powdered glasses using a TA Instruments equipment (model 2910). In order to determine nucleation rate versus isothermal temperature of heat treatment, bulk samples were quickly heated from room temperature to a nucleation temperature between T_g and crystallization temperature T_c, preliminary determined by DSC, at a $10\ \mathrm{K\ min^{-1}}$ heating rate. The nucleation stage was performed at this temperature for 20 min, then samples were quenched to room temperature. Then the DSC curves of the heat treated samples were recorded at $10\ \mathrm{K\ min^{-1}}$. All samples used in this study were cut from the same glass rod.

The NMR ^{19}F relaxation times measurements were carried out at a frequency of 36 MHz, by means of a home built pulsed NMR spectrometer. Spin–lattice relaxation times were determined using the progressive saturation method. Glass samples were cut into small pieces to fill the 4 mm diameter sample tubes.

After heat treatment, a x-ray diffraction analysis of the powered sample was carried out using Cu K-α radiation.

III. RESULTS AND DISCUSSION

A. Differential scanning calorimetry

Thermograms obtained for IZSB ($40InF_3$–$20ZnF_2$–$20SrF_2$–$20BaF_2$) glass samples are shown in Fig. 1. Curve (a) corresponds to an untreated sample, annealed below glass transition temperature T_g. Curves (b), (c), (d), and (e), refer to samples isothermally heated at 573, 613, 633, and 653 K, respectively.

DSC curves for samples (a)–(c) present a relaxation peak at T_g (573 K). The decrease of the intensity of this

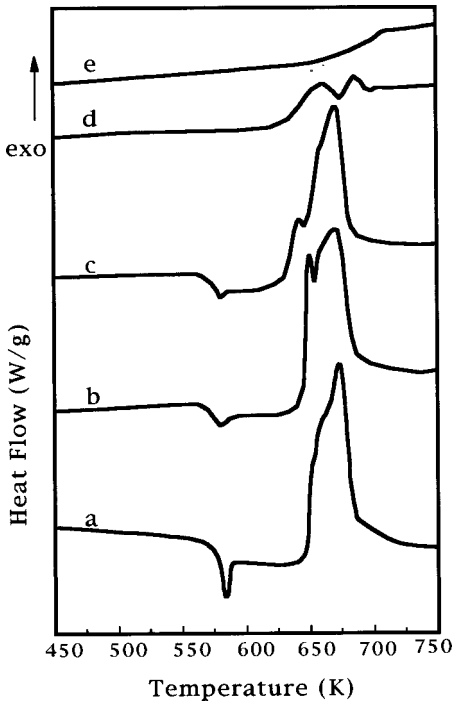

FIG. 1. DSC scans of powdered $40InF_3$–$20ZnF_2$–$20SrF_2$–$20BaF_2$ glass samples, for the base glass (a) and for samples annealed for 20 min at 573 K (b), 613 K (c), 633 K (d), and 653 K (e).

relaxation peak results from the decrease of the glass fictive temperature induced by the annealing stages.

This effect is lower for samples (b) and (c), which where cooled slowly; the furnace was switched off after heating, corresponding to a cooling rate much lower than the heating rate in the DSC scan ($10\ K\ min^{-1}$). The shift in the base line before and after T_g reflects the difference in the C_p of the solid and the liquid glass phases. The magnitude of this shift decreases if the sample is partly crystallized and does not exist later when crystallization is completed. From this it appears that samples (b) and (c) remain largely vitreous while the crystallization process of sample (d) is almost completed.

The crystallization peak of the untreated glass sample is complex and two shoulders may be observed before the maximum of the exothermic peak. Isothermal annealing changes the structure of the peak. The intensity of the first shoulder increases to the point that it appears as a distinct peak, and sharper in sample (b) than in sample (c). In the meantime, the position of the exothermic maximum remains nearly constant. The DSC scan of the sample (d) shows two broad exothermic peaks. The higher temperature one is likely to occur also in the (a), (b), and (c) scans.

The expected effect of the annealing stage above T_g is to induce extra nucleation and, in turn, to increase the number of crystals growing at a given temperature. Consequently, the crystallization peak height, which is assumed to be proportional to the concentration of nuclei,[13] might also increases. In addition, as more crystals are growing at the same time, overall crystallization is faster, and the maximum of the exothermic peak is shifted toward lower temperatures. The observation of the DSC scans in Fig. 1 suggests a more complex crystal growth mechanism.

The rules expressed above apply when a single phase is growing from nuclei generated during thermal treatment. In here, it may be assumed that there are four sets of crystalline phases involved in the devitrification process, associated to the four components of the exothermic peak. Note that we do not make any assumption about the crystallographic nature and the number of chemical compounds involved in the process.

Let us label these sets A, B, C, and D. In a first step the following transformation could occur from the liquid glass G

$$G \Rightarrow A + L_1, \tag{1}$$

where L_1 is the remaining liquid phase. Nuclei generated above T_g only form crystals belonging to A. Therefore, the height of the corresponding peak increases. This peak appears as a shoulder for sample (a) and becomes distinct in curve (b). However, some crystal growth takes place during annealing. When the annealing temperature increases, a part of the A crystals are already formed, and the enthalpy released on reheating is lower. This is consistent with the observation (see Fig. 1) that this first crystallization peak in (c) is located at a lower temperature, and also less pronounced.

In a second step, liquid L_1 which is unstable, also crystallizes. There are two possible mechanisms: either only remaining liquid is involved, according to the equation

$$L_1 \Rightarrow B + L_2, \tag{2}$$

where L_2 is the remaining liquid after B formation; or there is a chemical reaction involving the A phase

$$L_1 + A \Rightarrow B + L_2. \tag{3}$$

This remaining liquid finally crystallizes, leading to the C phase

$$L_2 \Rightarrow C. \tag{4}$$

According to this mechanism, the A phase grows first in samples (a), (b), and (c) giving a residual liquid L_1. As the annealing stage does not produce nuclei for phase B, nucleation is homogeneous and there is no variation in the position of the two next crystallization exothermic. In particular, no significant amount of L_2 liquid crystallizes prior to the DSC scan. For sample (d), the higher annealing temperature induces the partial crystallization of the L_2 liquid, and the corresponding crystals, which remain in glass, act as nucleating sites for the end of the devitrification process. As a consequence, the peak is shifted to a lower temperature.

The last exothermic, which appears more clearly in sample (d), may correspond to the final crystallization stage (phase D) of an hypothetical residual liquid, or to the result of a solid state reaction, involving some of the crystalline compounds produced in the devitrification process. The DSC curve of sample (e) could suggest that some further transformation occurs beyond 700 K. This hypothesis is not contradictory with the other DSC scans, but needs a more accurate study to be confirmed.

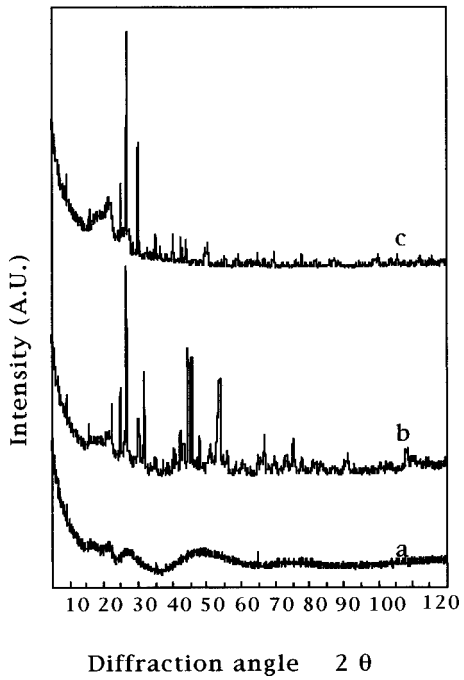

FIG. 2. X-ray diffractograms of powdered $40InF_3$–$20ZnF_2$–$20SrF_2$–$20BaF_2$ glass samples treated at 633 K (a), 653 K (b), and 673 K (c).

B. X-ray diffraction

In order to obtain additional information on the crystallizing phases, we also performed x-ray diffraction measurements. Figure 2 shows the XRD powder patterns of samples, heat treated in air at 633 K (a), 653 K (b), and 673 K (c). The glass (a) exhibits the broad characteristic bands of the amorphous state. In fact, this pattern also encompasses the x-ray diffusion of the polymeric sample holder. The heat treatment at 653 K has produced many peaks, some of which could be assigned to a mixture of metastable phases. The predominant phases in patterns (3b) and (3c) can be tentatively assigned as BaF_2, ZnF_2, In_2O_3, $BaZnF_4$, InOF, and γ-InF_3. The x-ray pattern of the treated sample at 653 K contains some peaks that are not present in the sample treated at 673 K. This is consistent with the hypothesis expressed above, which suggests that some solid phase transformation could occur at high temperature. This behavior is similar to that of fluorozirconate glasses, in which BaF_2 and $BaZrF_6$ have also been identified by XRD, for heat treated samples,[14] with a β–α solid state transition.

C. Nuclear magnetic resonance

NMR is an effective technique for obtaining information about the microscopic character of ion motion in fast ionic conductors (fluoride glasses, solid, and polymer electrolytes), due to the effects that such motion has on the nuclear spin–relaxation times.[15–17] In particular, fluoride glasses have been investigated by ^{19}F NMR for more than 15 years. Most of the works were focused on ZrF_4-based glasses, concerning temperature dependence of the ^{19}F linewidth and nuclear relaxation times. NMR techniques are very suitable for studying fluoride glasses since ^{19}F is the only stable isotope of fluorine, and has a nuclear spin of 1/2 (gyromagnetic ratio value $\gamma = 4.0059$ kHz/G) and therefore no quadrupolar moment.

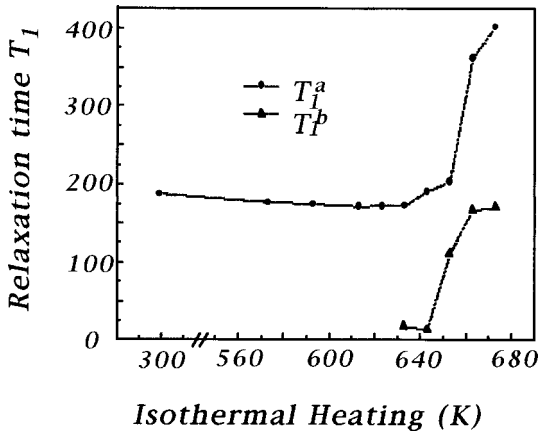

FIG. 3. ^{19}F Nuclear spin–lattice relaxation time (T_1) as a function of the thermal treatment temperature of the $40InF_3$–$20ZnF_2$–$20SrF_2$–$20BaF_2$ glass samples. Measurements were made at room temperature at the Larmor frequency of 36 MHz.

Earlier NMR studies on ZrF_4-based glasses focused on the determination of the fraction of mobile fluorine ions as a function of temperature, and of the activation energies, from the temperature dependence of the ^{19}F linewidths,[18,19] and also to show the existence of different fluoride sublattices in some glasses.[20,21] Many studies of the temperature dependence of the ^{19}F spin–lattice relaxation times in fluorozirconate glasses have also been reported.[14,22–25] These nuclear relaxation results were interpreted in terms of two contributions; a first one dominating below the glass transition temperature T_g, where the spin relaxation process is attributed to low-frequency excitation of disorder modes, and a second one at high temperatures, where the diffusive ionic motions are responsible for the relaxation process.[14,24,25] Progress in NMR characterization of ionic transport and relaxation in glasses was recently reviewed by Kanert and co-workers.[15] In general, little attention has been paid to NMR studies concerning the crystallization process occurring above the glass transition temperature. Some measurements of the ^{19}F spin–lattice relaxation time, bellow and above T_g, have been reported in ZBLALi and CLAP fluoride glasses.[25]

Fluoride glasses based on InF_3 were also studied by NMR. Ignat'eva and co-workers reported an IR, Raman, and NMR spectroscopy study in InF_3–PbF_2–MF_2 (M=Ba, Zn, and Mn) glasses. The ^{19}F NMR spectra show the occurrence of two components reflecting the inhomogeneity of the fluorine subsystem in these glasses.[26] Recently, we reported the measurements of the temperature and frequency dependence of ^{19}F nuclear relaxation times, for fluoride glasses based on ZrF_4 and InF_3. The measurements were performed from 185 to 1000 K. Results show clearly two distinct relaxation behaviors, where one mechanism dominates below T_g and the other, responsible for the spin–lattice relaxation, above T_g.[27]

Measurements, at room temperature, of the fluorine ^{19}F spin–lattice relaxation time, T_1, as a function of the isothermal heat treatment of the glass are shown in Fig. 3. The first

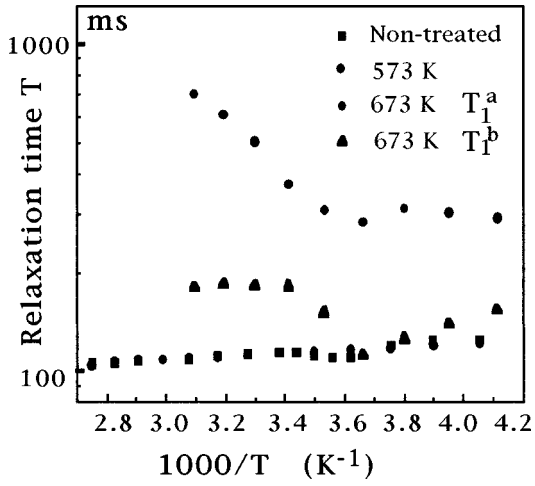

FIG. 4. Temperature dependence of the ^{19}F nuclear spin–lattice relaxation time (T_1) in the glass $40InF_3$–$20ZnF_2$–$20SrF_2$–$20BaF_2$, measured at the Larmor frequency $\omega_0 = 36$ MHz.

point, at 300 K, corresponds to untreated glass sample. For samples heat treated at temperatures lower than 628 K, the recovery of the nuclear magnetization toward equilibrium is well described by a single exponential curve, and only one relaxation time T_1 was observed. For samples heat treated at 623 K, it was observed that the relaxation time slightly decreases, from 187 to 171.8 ms. For samples heat treated above 628 K, the NMR relaxation is adequately described by the sum of two exponential curves, associated with two relaxation times, denoted by T_1^a and T_1^b. Both resulting relaxation times increase with increasing treatment temperature. For samples heat treated near the crystallization temperature (673 K), $T_1^a = 361.8$ ms and $T_1^b = 170$ ms.

Fluorine spin–lattice relaxation times as a function of the temperature, for the untreated sample and treated samples at 573 and at 673 K are shown in Fig. 4. For the untreated glass sample and for the one treated at 573 K, the relaxation time T_1 does not change appreciably in the temperature range between 240 and 365 K. For the sample annealed at 673 K, the relaxation time T_1^b changes very little with temperature, between 240 and 325 K, indicating the slow mobility of the ions in this temperature range. Furthermore, T_1^a increases at temperatures above 274 K, indicating the existence of a broad minimum around this temperature. The observed temperature dependence of T_1^a can indicate a relaxation process dominated by the fluorine ionic diffusion. When temperature increases, ion diffusion becomes appreciable, and the nuclear moment will be subject to a time dependent random magnetic field, which causes nuclear magnetisation to relax dynamically. In particular, for a spin-1/2 nucleus, such as ^{19}F, the nuclear relaxation results from the modulation of the nuclear spin dipole–dipole interaction by the ionic motions. In most cases, the relaxation rate will depend on temperature through an effective correlation time, τ, expressed by an Arrhenius law, $\tau = \tau_0 \exp(E_a/k_B T)$, which introduces the activation energy E_a, and the prefactor τ_0. Considering a harmonic approximation for the periodical potential, in which the ion moves, the attempt frequency τ_0^{-1} can be interpreted as a vibrational frequency, of the order of an optical phonon frequency, 10^{12} to 10^{13} s^{-1}. This correlation time defines the time scale for the changes of the local magnetic field, experienced by the resonant nucleus, and can be interpreted as the characteristic time of the transport processes.

The data of T_1^a vs T^{-1} for treated sample at 673 K (Fig. 4) exhibits a broad asymmetric minimum near 274 K, very similar to that determined for ternary compounds, with the fluorite structure,[16] and also for fluoride glasses at elevated temperatures where, as mentioned above, the diffusive fluorine ionic motions are responsible for the temperature dependence of the nuclear relaxation.[15] The origin of the asymmetric minimum was attributed to a fast decay of the spin correlation function, where for a lower time, t, compared to τ, decays faster than for the phenomenologically assumed exponential form, $\exp(-t/\tau)$, characteristic of the Bloembergen–Purcell–Pound (BPP) model.[16] As discussed quantitatively in Ref. 16, this effect enhances the relaxation rate (T_1^{-1}) at low temperatures (where $\omega_0 \tau \gg 1$), and breaks the symmetry of the V-shaped T_1 vs $1/T$ curves, predicted by the BPP model. By contrast, for very short correlation times ($\omega_0 \tau \ll 1$), i.e., for temperatures above the spin–relaxation minima, τ governs the decay of the spin–correlation function, as in the BPP model. This interpretation allows us to determine the activation energy of the fluorine diffusion motion. From the data of T_1^a vs T^{-1} (Fig. 4), since $\omega_0 = 2.26 \times 10^8$ rad/s, the following parameters can be obtained: $E_a = 0.18 \pm 0.01$ eV and $\tau_0 = 1.5 \pm 0.8 \times 10^{-12}$ s. This value of activation energy is in good agreement with the one obtained from ^{19}F NMR, for others fluoride glasses[13] and fluoride ionic conductors.[25] The existence of a distribution of the activation energies in disordered systems could well explain the asymmetric T_1 minima. Disorder, in the present case, arises from the random occupation of the cationic site in the different fluoride phases of the annealed samples. Such a disordered structure might confront the moving ion with different paths (i.e., barrier heights), leading to an inhomogeneous diffusion process. As discussed in Ref. 16, the hypothesis of a distribution of barrier heights is qualitatively equivalent to the nonexponential correlation function.

Concerning the significance of our measurements of ^{19}F relaxation, on glasses heat treated above 628 K (Fig. 3), it can be concluded that the magnetic interactions which are important in ''pure'' (free of paramagnetic impurities) fluoride glasses are: (a) dipole–dipole coupling of like spins (F–F) and (b) dipole–dipole couplings of unlike nuclear spins (F–In, F–Zn).[28]

For a system of spin-1/2 pairs (as ^{19}F–^{19}F) in contact with a heat bath at temperature T, and under a magnetic field $B = \omega/\gamma$, the spin–lattice relaxation rate can be described by

$$T_1^{-1}(\omega_0, \tau) = AJ(\omega_0, \tau), \tag{5}$$

where A is the measure of the dipole–dipole interaction, and determined by the structural geometry and the number of interacting nuclei, $J(\omega_0, \tau)$ is a sum of spectral densities, depending on Larmor frequency and some parameters which characterizes the motion. In viscous material, the correlation time τ is proportional to the viscosity and the inverse of the temperature, $\tau \propto \eta/T$.[29]

According to the DSC and XRD results discussed above, liquid and different metastable growing crystalline phases are dispersed in the vitreous matrix for glass samples heat treated above 628 K. It is well known that the viscosity of ZrF_4 glasses increases rapidly with decreasing temperature, approaching to 10^{12} Pa s, at the glass transition temperature, and to $10^{-2}-10^{1}$ Pa s, at temperatures above T_c.[30] Choi and Frischat also observed that the density increases with the crystalline phase content, during the crystallization process of ZrF_4-based glasses.[31] All these physical changes occurring during the crystallization process, added to the difference in the mobility of the fluorine ions in such emergent crystalline phases, might affect the A and the $J(\omega_0,\tau)$ terms in Eq. (5). Crudely, the decrease of the viscosity, observed in the fluoride glass samples treated at high temperatures, can explain qualitatively the tendency of the spin–lattice relaxation of the samples treated above 628 K (Fig. 3).

From the condition of the relaxation minimum of the T_1 at 274 K, $\omega_0\tau\approx 0.6$,[29] one can calculate the correlation time $\tau=4\times10^{-9}$ s, for the sample at 673 K (Fig. 4). This value is in agreement with the correlation time obtained from the viscosity value of the glass ($\approx$1 Pa s), by using the simple Einstein relation for viscous liquids,[29] assuming F–F distances of about 2.3 Å, as calculated for the InF_6 unit size.[26]

IV. CONCLUSIONS

This work was centered upon the crystallization and nucleation processes occurring in a fluoroindate glass samples, annealed between glass transition and crystallization temperatures. Our approach consisted mainly, in collecting data from three different techniques, DSC, NMR and XRD, in order to obtain more information concerning to crystallization and nucleation processes. The heat treatments of the glass samples give rise to a broad exothermic peak, encompassing several crystallization peaks on the DSC scans. A possible mechanism which was proposed for the overall transformation is consistent with XRD results.

The ^{19}F spin–lattice relaxation is clearly influenced by the crystallization process. The NMR relaxation is described by two time constants, for the glass samples annealed above 638 K. Experimental results make clear the fast ion motion in the glass samples treated at 673 K. The activation parameters (E_a,τ_0) obtained from the temperature dependence of T_1 are consistent with those reported in others fluoride ionic conductors.

ACKNOWLEDGMENTS

The financial support of the Capes-Cofecub, Pronex, CNPq, and the Fapesp (Brazil) is gratefully acknowledged.

[1] F. Gan, J. Non-Cryst. Solids **184**, 9 (1995).
[2] Y. Messaddeq, A. Delben, M. A. Aegerter, A. Soufiane, and M. Poulain, J. Mater. Res. **8**, 885 (1993).
[3] A. B. Seddon, D. L. Williams, and A. G. Clare, Phys. Chem. Glasses **31**, 64 (1990).
[4] S. Y. Choi and G. H. Frischat, J. Non-Cryst. Solids **129**, 133 (1991).
[5] A. Elyamani, E. Snitzer, R. Pafchek, and G. H. Sigel, J. Mater. Res. **7**, 1541 (1992).
[6] A. B. Seddon and A. V. Cardoso, Phys. Chem. Glasses **35**, 137 (1994).
[7] P. Santa-Cruz, D. Morin, J. Dexpert-Ghys, A. Sadoc, F. Glas, and F. Auzel, J. Non-Cryst. Solids **190**, 238 (1995).
[8] S. J. L. Ribeiro, P. Goldner, and F. Auzel, J. Non-Cryst. Solids **219**, 176 (1997).
[9] M. Barico, L. Battezati, M. Braglia, G. Cocito, M. Gava, J. Kraus, and S. Mosso, J. Non-Cryst. Solids **213&214**, 79 (1997).
[10] T. Iqbal, A. N. Kayani, M. R. Shariari, and G. H. Sigel, J. Non-Cryst. Solids **213&214**, 79 (1997).
[11] J. Malék, Y. Messaddeq, S. Inoue, and T. Mitsuhashi, J. Mater. Sci. Lett. **30**, 3082 (1995).
[12] J. Zhu, Z. Bo, and D. Dong, J. Non-Cryst. Solids **47–51**, 201 (1996).
[13] C. S. Ray and D. E. Day, J. Am. Ceram. Soc. **73**, 439 (1990).
[14] O. Kanert, A. Hackmann, R. Kuchler, and K. L. Ngai, J. Non-Cryst. Solids **172–174**, 1424 (1994).
[15] O. Kanert, J. Dieckofer, and R. Kulchler, J. Non-Cryst. Solids **203**, 252 (1996).
[16] J. P. Donoso, L. N. Oliveira, H. Panepucci, A. Cassanho, and H. Guggenheim, J. Phys. C **19**, 963 (1986).
[17] J. P. Donoso, T. J. Bonagamba, H. Panepucci, L. N. Oliveira, W. Gorecki, C. Berthier, and M. Armand, J. Chem. Phys. **98**, 10026 (1993).
[18] J. Senegas, J. M. Reau, H. Aomi, P. Hagenmuller, and M. Poulain, J. Non-Cryst. Solids **85**, 315 (1986).
[19] S. Estalji, R. Kulchler, O. Kanert, R. Bolter, H. Jain, and K. L. Ngai, J. Phys. (Paris), Colloq. **C2**, 159 (1992).
[20] J. M. Bobe, J. Senegas, J. M. Reau, and M. Poulain, J. Non-Cryst. Solids **162**, 169 (1993).
[21] S. Berger, J. Roos, D. Brinkmann, and B. V. R. Chowdari, Solid State Ionics **86–88**, 475 (1996).
[22] A. Uhlherr, D. R. MacFarlane, and T. J. Bastow, J. Non-Cryst. Solids **123**, 42 (1990).
[23] S. Estalji, O. Kanert, J. Steinert, H. Jain, and K. L. Ngai, Phys. Rev. **43**, 7481 (1991).
[24] O. Kanert, J. Steinert, H. Jain, and K. L. Ngai, J. Non-Cryst. Solids **131**, 1001 (1991).
[25] R. Kulchler, O. Kanert, M. Fricke, H. Jain, and K. L. Ngai, J. Non-Cryst. Solids **172–174**, 1373 (1994).
[26] L. N. Ignat'eva, T. F. Antokhina, V. Ya. Kavun, S. A. Polishchuk, E. A. Stremousova, E. B. Petrova, V. M. Buznik, and S. G. Bakhvalov, Glass Phys. Chem. **21**, 53 (1995).
[27] T. Auler, P. L. Frare, C. J. Magon, M. A. Ferraz, J. P. Donoso, Y. Messaddeq, and A. A. S. T. Delben, J. Non-Cryst. Solids (to be published).
[28] J. Boyce and B. A. Huberman, Phys. Rep. **51**, 189 (1979).
[29] A. Carrington and A. D. McLachlan, *Introduction to Magnetic Resonance* (Harper & Row, New York, 1967).
[30] K. Matusita, M. Koide, and T. Komatsu, J. Non-Cryst. Solids **140**, 141 (1992).
[31] S.-Y. Choi and G. H. Frischat, J. Non-Cryst. Solids **129**, 133 (1991).